JOURNAL OF APPLIED POLYMER SCIENCE VOL. III, ISSUE NO. 9, PAGES 257–265 (1960)

Mechanism of Lubricant-Extrusion of Teflon* TFE–Tetrafluoroethylene Resins†

G. R. SNELLING and J. F. LONTZ

Polychemicals Department, E. I. du Pont de Nemours Company, Inc., Du Pont Experimental Station, Wilmington, Delaware

Lubricant extrusion is a method used for forming Teflon* tetrafluoroethylene resins derived from dispersion and admixed with lubricants into wire coating, tubing, and tape.[1–3] The extrusion involves the elongation of the approximately spherical dispersion resin into a fibrous structure[4] during passage through an extruder die. The elongation confers on the extrudates sufficient tensile strength to withstand stresses during subsequent drying and sintering operations. In contrast to conventional melt extrusion, the behavior departs from the usual features of viscous flow and in lieu thereof requires consideration of particulate deformation. This paper therefore proposes a stress–strain model for the extrusion process that can be used to develop equations of flow which are in harmony with the observed relations between pressure, flow rate, die dimensions, and time of extrusion.

THEORETICAL CONSIDERATIONS

Stress–Strain Model for Lubricant Extrusion

A stress–strain relation suitable for representing the behavior of the lubricant–resin mixture in total compression, such as in an extrusion machine, must allow for two important experimental observations.

(*a*) The extrudates are considerably stronger than the preform or billet charged to the extrusion machine. This effect can be regarded as strain-hardening, as it can be shown that the tensile strength of the extrudate is proportional to the strain (reduction of area) imposed during the course of extrusion. A practical appreciation of this hardening may be obtained by noting the greatly increased stiffness near the apex of heels removed from an extrusion machine die. The additional observation that the preforms have enough strength to hold their shape might lead one to suppose that there is an appreciable yield strength of the unsheared paste. However, experiment shows the increase of strength is due to fibering and is so large that the initial yield strength of the preform is comparatively negligible.

(*b*) The familiar viscous resistance of conventional melt extrusion is apparent as a dependence of the extrusion pressure on both the flow rate and the die angle.

From the above general observations and ensuing detailed rheometer experiments, a maximum shearing stress–maximum shearing strain relation in total compression has been found suitable in the general expression:

$$\tau_{max} = C\gamma_{max}^{n} + \eta(d\gamma_{max}/dt)^{m} \qquad (1)$$

where τ_{max}, γ_{max}, and t are the maximum shearing stress, maximum shearing strain, and time, respectively, and C, n, η, and m are derivable material constants. (The shearing strain used in the analysis of large deformation is the so-called logarithmic shearing strain, in which strain increments are calculated with respect to the instantaneous length rather than the original length as in small deformations. Further information on the use and mathematical properties of logarithmic strain is given in References 5–7.) The first right-hand term, as a power function of the maximum shearing strain, is used to describe the increment of the maximum shearing stress due to strain hardening.[5] The second right-hand term, a power function of the strain rate, is used to describe the variation of stress due to strain rate variation. The yield stress of

* Registered trademark of E. I. du Pont de Nemours & Co., Inc., for their fluorocarbon resins, including the TFE (tetrafluororesin) resin described here.

† Presented before the Division of Polymer Chemistry, American Chemical Society Meeting, Chicago, Illinois, September 1958.

the unsheared paste τ_y is neglected, but this could be accounted for by adding τ_y to the right-hand side of eq. (1). The material constants C, n, η, and m are to be experimentally evaluated.

Equation of Flow for Lubricated Resin in a Conical Die Channel

To derive an equation of flow for the conical die of an extruder it is necessary to have a knowledge of the deformation pattern therein. Experiment shows (as will be detailed later) that the deformation pattern is described suitably by the statement that particles equidistant from the die virtual apex of the die have equal velocities directed towards the virtual apex. Consider now the volume element shown in Figure 1 which is bounded by spherical surfaces at radius r and $(r + dr)$ and by four planes which when projected pass through the virtual apex. The above statement defining the deformation pattern implies that the volume element deforms in such a way that its bounding surfaces remain parallel to their previous positions. In addition, the fact that the element does not rotate or deviate from its straight path implies that the stresses on its faces are purely normal stresses; in fact, the radial direction and the directions normal to the four planes are principal directions with principal stresses δ_r and δ_α, respectively. The element is, during extrusion, confined to the sector bounded by the projection through the virtual apex of its four plane faces. The radial and normal stresses on the sector are identical to those on any similar section; consequently, the stress analysis requires the consideration of one sector only. The absence of shearing stresses on the plane faces of the element is in accordance with experiment showing die wall friction to be negligible, as will be described later.

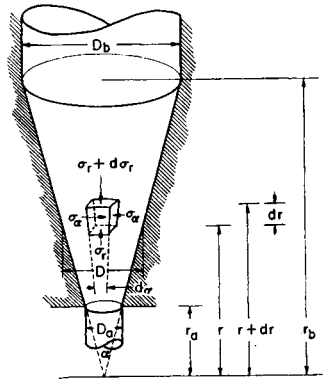

Fig. 1. Volume element used in stress analysis.

A force balance in the r direction of the element in Figure 1 (neglecting differentials of higher order) gives the radial stress gradient $d\delta_r/dr$ in terms of the stresses δ_r and δ_α normal to the radial direction and the perpendicular to the radial direction, respectively:

$$d\delta_r/dr = 2(\delta_\alpha - \delta_r)/r \tag{2}$$

The relation between the stresses δ_r, δ_α and the maximum shearing stress is[6]

$$\delta_\alpha - \delta_r = 2\tau_{\max} \tag{3}$$

Suitable combination of eqs. (1), (2), and (3) gives the differential equation of flow:

$$d\delta_r/dr = 4\tau_{\max}/r$$
$$= (4/r)[C\gamma_{\max}{}^n + \eta(d\gamma_{\max}/dt)^m] \tag{4}$$

It is apparent from eq. (4) that the die pressure drop ΔP

$$\Delta P = \int_{r=r_a}^{r=r_b} d\delta_r$$

may be expressed as the sum of two components: ΔP_{SH}, a component due to strain hardening, and ΔP_{SR}, a component due to viscous resistance of the resin–lubricant mixture:

$$\Delta P = \Delta P_{SH} + \Delta P_{SR}$$

where

$$\Delta P_{SH} = \int_{r=r_a}^{r=r_b} [4C/r][\gamma_{\max}{}^n\, dr] \tag{5}$$

and

$$\Delta P_{SR} = \int_{r=r_a}^{r=r_b} [4\eta/r][d\gamma_{\max}/dt]^m dr \tag{6}$$

Here r_a and r_b are, respectively, the radial distances from the die apex of the die orifice and die entrance.

To integrate eqs. (5) and (6) it is necessary to express the logarithmic shearing strain $\gamma_{\max}$ and shearing strain rate $d\gamma_{\max}/dt$ in terms of the linear radial strains

$$d\bar{\epsilon}_r = drd\alpha/rd\alpha = dr/r$$

Providing the volume of the element remains constant,

$$d\bar{\epsilon}_{\mathrm{I}} + d\bar{\epsilon}_{\mathrm{II}} + d\bar{\epsilon}_{\mathrm{III}} = 0$$

and, since

$$d\bar{\epsilon}_{\mathrm{II}} = d\bar{\epsilon}_{\mathrm{III}} = d\bar{\epsilon}_\alpha$$

then

$$d\bar{\epsilon}_I = d\bar{\epsilon}_r = 2d\bar{\epsilon}_\alpha$$

and

$$\begin{aligned}\gamma_{max} &= \bar{\epsilon}_I - \bar{\epsilon}_{III} \\ &= -3\int d\bar{\epsilon}_\alpha \\ &= -3\int dr/r \end{aligned} \quad (7)$$

Here, ϵ_r and ϵ_α are the linear logarithmic strains in the radial direction and perpendicular to the radial direction, respectively; ϵ_I, ϵ_{II}, and ϵ_{III} are the major, intermediate, and minor principal linear logarithmic strains, respectively.

The shearing strain rate $d\gamma_{max}/dt$ is expressed in terms of the linear strain by noting that the velocity of a point on a spherical surface at distance r from the apex is

$$\begin{aligned}-dr/dt &= Q/(\text{area of surface}) \\ &= Q/2\pi(1 - \cos\alpha)r^2 \end{aligned} \quad (8)$$

where Q is the extruder volumetric flow rate and α is the die semiangle. From eqs. (7) and (8) we have

$$\begin{aligned}d\gamma_{max}/dt &= -3dr/rdt \\ &= 3Q/2\pi(1 - \cos\alpha)r^3 \end{aligned} \quad (9)$$

By substituting for $d\gamma_{max}/dt$ from eq. (9) into eq. (6) the latter is integrated to

$$\Delta P_{SR} = [4\eta/3m][3Q/2\pi(1 - \cos\alpha)r_b^3]^m \times [(r_b/r_a)^{3m} - 1] \quad (10)$$

Before integrating eq. (5) it is necessary to reflect on the physical meaning of the strain hardening component. The strain of any element depends on the distance it has traveled in the die. Normally, for the *steady-state extrusion*, an element at radius r will have suffered deformation in traveling from the die entrance at radius r_b. However, in the early unsteady-state extrusion, elements originally resident in the die at a radial distance from the apex r_i at time $t = 0$ will reach radius r from the apex at time $t = t$. The relation between r_i and r, the equation of continuity for the die, is obtained by integrating eq. (8) to give

$$r_i^3 = 3Qt/2\pi(1 - \cos\alpha) + r^3 \quad (11)$$

For unsteady-state extrusion, the strain at radius r is, from eq. (7)

$$\gamma_{max} = 3\int_{r_i}^{r} dr/r = 3\ln(r_i/r) \quad (12)$$

and, from eqs. (5) and (12), we have

$$\Delta P_{SH} = \int_{r_a}^{r_b} (4C/r)[3\ln(r_i/r)]^n dr \quad (13)$$

Equation (13) cannot be integrated analytically. A solution may be obtained by numerical integration in conjunction with eq. (11) which is used to obtain r_i. It should be noted that the unsteady state ceases when $r_i = r_b$, and this is the maximum permissable value of r_i. The corresponding time is

$$t = (2\pi/3Q)(1 - \cos\alpha)(r_b^3 - r^3)$$

For steady-state extrusion, eq. (13) is integrated after putting $r_i = r_b$ to give

$$\Delta P_{SH} = [4C/3(n + 1)][3\ln(r_b/r_a)]^{n+1} \quad (14)$$

The following two equations permit simplification of the flow equations.

The relation between the radial distance of an element and the corresponding diameter D in die cone or extruder cylinder is

$$\sin\alpha = D/2r = D_a/2r_a = D_b/2r_b \quad (15)$$

where D_a and D_b are the diameters of the die orifice and entrance, respectively.

At high reduction ratios,

$$(r_b/r_a)^{3m} - 1 \simeq (r_b/r_a)^{3m} \quad (16)$$

Flow Equations

The *steady-state pressure drop* is found from eqs. (10), (14), (15), and (16) to be

$$\begin{aligned}\Delta P &= \Delta P_{SH} + \Delta P_{SR} \\ &= [4C/3(n + 1)][3\ln(D_b/D_a)]^{n+1} + [4\eta/3m] \\ &\quad \times [12Q\sin^3\alpha/\pi(1 - \cos\alpha)D_a^3]^m \end{aligned} \quad (17)$$

The *maximum shearing stress* at diameter D in the cone and for steady-state extrusion is, from eqs. (1), (9), (12), and (15),

$$\begin{aligned}\tau_{max} &= \tau_{SH} + \tau_{SR} \\ &= C[3\ln(D_b/D)]^n \\ &\quad + \eta[12Q\sin^3\alpha/\pi(1 - \cos\alpha)D^3]^m \end{aligned} \quad (18)$$

where τ_{SH} and τ_{SR} are components of maximum shearing stress due to strain hardening and strain rate, respectively.

The *maximum shearing strain* at diameter D in the cone and for steady-state extrusion is, from eqs. (12) and (15),

$$\gamma_{max} = 3\ln(D_b/D) \quad (19)$$

Extruder Wall Friction

The preceding analysis of conditions in the die assumes slip of the paste and negligible friction at the die wall. In practice it appears to be difficult

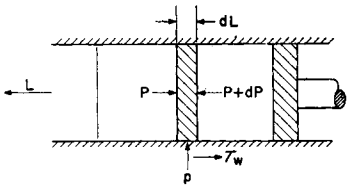

Fig. 2. Dimensions in extruder cylinder analysis.

to obtain measurements of friction in the die. For this reason friction measurements were made in the extruder cylinder instead. The following analysis shows how the coefficient of friction at the cylinder wall can be deduced from pressure drop measurements.

Consider (Fig. 2) the volume element of diameter D and thickness dL. The coefficient of friction μ is defined as the shear force at wall/normal force at wall or

$$\mu = \pi DdL\tau_w/\pi DdLp = \tau_w/p \qquad (20)$$

where L is the cylinder length between probes A and B, τ_w is the shearing stress at the cylinder wall, and p is the normal pressure at the cylinder wall. Resolving forces in the L direction, we obtain:

$$(\pi D^2/4)dP = \pi DdL\tau_w$$

$$\therefore \quad \tau_w = (D/4)(dP/dL) \qquad (21)$$

Eliminating τ_w between eqs. (20) and (21) we obtain

$$\mu = (D/4p)(dP/dL) \qquad (22)$$

Conceivably, with some lubricant mixtures there will be a difference, at a given L between the axial pressure P and that transmitted normally to the wall. The pressure difference ΔP_0 defined as

$$P - p = \Delta P_0 \qquad (23)$$

is strictly a material property. However ΔP_0 must be expected to vary with (a) the pressure level, because the preform density and therefore the area of contacting surfaces in the resin grains must depend on the pressure level and (b) change of particle shape occasioned by shear of particles. If it is found by experiment that there is little pressure drop along the extruder cylinder and the resin grains are not deformed in the cylinder then an assumed constancy of ΔP_0 for any one experiment is justified. With this in mind p may be eliminated between eqs. (22) and (23) to give

$$dP/(P - \Delta P_0) = 4\mu(dL/D)$$

Integration between limits

$$P = P_1 \quad L = 0$$
$$P = P_2 \quad L = L$$

yields

$$\ln [(P_1 - \Delta P_0)/(P_2 - \Delta P_0)] = 4\mu(L/D) \qquad (23a)$$

Defining $\Delta P_c = P_1 - p_2$ and noting $P_2 - \Delta P_0 = p_2$, then eq. (23a) may be written

$$\ln [1 + (\Delta P_c - \Delta P_0)/p_2] = 4\mu(L/D) \qquad (24)$$

The approximation

$$\ln [1 + (\Delta P_c - \Delta P_0)/p_2] \rightarrow (\Delta P_c - \Delta P_0)/p_2$$

introduces an error as shown in Table I.

TABLE I

$(\Delta P_c - \Delta P_0)/p_2$	Error, %
0.05	2.4
0.10	4.9
0.15	7.3

Use of the approximation yields for eq. (24)

$$\Delta P_c = 4\mu(L/D)p_2 + \Delta P_0 \qquad (25)$$

EXPERIMENTAL

In order to determine if the preceding equations are suitable for correlating the extrusion variables experimental extrusions were made as described below.

Equipment and Materials

The rheometer used (Fig. 3) is a small ram extruder having a $1^1/_4$-in. diameter and 6-in. long cylinder. The piston can be moved at a precise constant rate or varied in speed to deliver 0–2 in./min. of lubricated Teflon tetrafluoroethylene resin by means of a variable drive system. The pressure at the piston face and at one location in the cylinder wall can be measured by accurately calibrated electrical sensing elements (A and B in Figure 3). A set of interchangeable 30° included angle conical dies provide reduction ratios R from 44.2 to 1507. The reduction ratio $R = (D_b/D_a)^2$ is defined as the cylinder cross-sectional area/orifice cross-sectional area. Teflon 6, lubricated as described by De Young[3] with Soltrol-130 (a mixture of branched-chain aliphatic hydrocarbons of boiling range 170–210°C., Phillips Petroleum Company), was used exclusively.

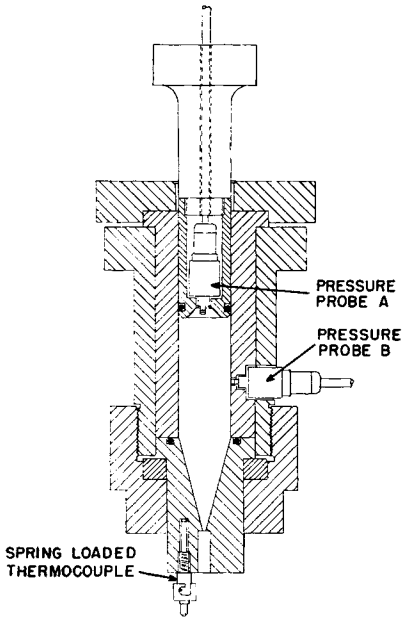

Fig. 3. Rheometer die assembly ($1^1/_4$-in. diameter).

Deformation Patterns

To test the hypothesis concerning the particle kinematics involved in the theoretical analysis, extrusions were made of preforms having layers of pigmented resin. The die heels were sliced down the center and the distortion of the layers (Fig. 4) assessed by measuring the distance of each layer from the virtual apex of the die at the center and at the die wall. The layers sometimes extruded in a lopsided manner, presumably owing to poor leveling in the preparation of the billet. Such extrusions were not used for measurement. Additionally, elastic recovery of the heels when removed from the die resulted in the measured distortion being somewhat less than the true distortion in the die. Recovery also had the effect of pulling the colored die layers apart somewhat.

Friction Measurement

To obtain values of the coefficient of friction by experiment extrusion runs were made while recording the pressure at probes A and B (Fig. 3). The rheometer piston was moved forward at constant rate so as to reduce the distance L between the probes from 3–4 in. to zero. This procedure was used with pastes of lubricant concentration of 0–19% and with various cylinder pressure levels. The latter was adjusted by selection of a suitable die orifice diameter for the pressure level required.

Pressure–Flow Rate Measurements

Extrusions were made at constant flow rate and the pressure at the piston face measured by Probe A. The extrusions were chosen so as to provide a steady-state pressure versus flow-rate plot for each die and paste compositions of 15, 17, 19, and 21 wt.-% of Soltrol. The steady state pressure was estimated from the pressure probe record after allowing sufficient time for the discharge of the original die contents during which time a rising extrusion pressure was observed.

RESULTS

A comparison of the experimental points obtained from the colored layer deformations with the line calculated from the radial flow hypothesis is given in Figure 5. The actual deformations are all slightly less than expected from the calculation; this is consistent with the observed recovery of the heels on removal from the die. The experiment provides only a crude verification of the assumed

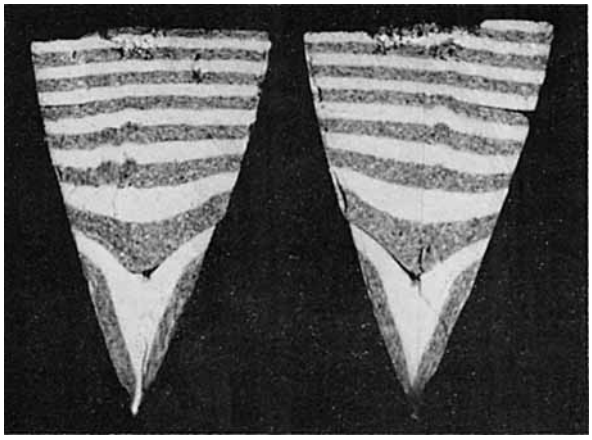

Fig. 4. Die heels showing distortion of pigmented layers.

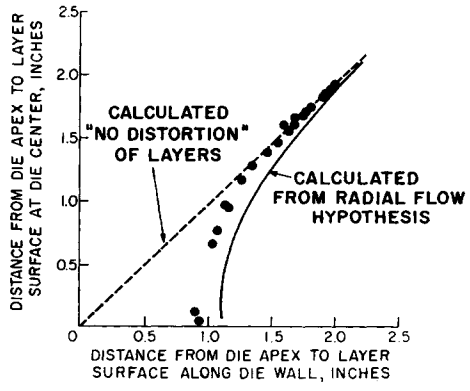

Fig. 5. Distortion of surfaces in die. Die used: $2\alpha = 30°$ angle; reduction ratio $R = 400$.

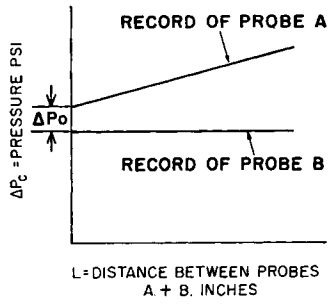

Fig. 6. Form of pressure record in friction measurements.

flow pattern, but serves to demonstrate that the radial flow hypothesis is not inconsistent with experiment.

The pressure records obtained in the friction measurements have the form shown in Figure 6. From these records the coefficient of friction was calculated by use of eq. (25); this yielded the values shown in Table II. When 17 or 19% Soltrol lubricant was used, the pressure records for both probes were identical. The sensitivity of the measurements is such that for these cases the coefficient of friction is less than 0.001. Runs made with 10, 5, and 0% Soltrol gave higher values of μ as shown, the measurement of 0% lubricant being comparable with existing data[8] for Teflon powders. In the runs with 10% or less lubricant, ΔP_0 was of appreciable magnitude, as also shown in Table II. The coefficient of friction is apparently decreased with increasing load judging by the results at 10 and 5% lubricant. This is also consistent with previous measurements.[9]

TABLE II
Coefficient of Friction for Lubricated Teflon 6

Soltrol lubricant, wt.-%	Downstream normal pressure, psi	Coefficient of friction	ΔP_0, psi
19	9700		
	4000	[a]	[a]
17	5000		
10	6000	0.007	1000
	980	0.024	200
5	4500	0.027	800
	1900	0.036	650
0	6400	0.043	1800

[a] Too small to be estimated.

Steady-state pressure versus flow rate plots were used to evaluate the constants C, n, η, and m by a slope-and-intercept method which is apparent on inspection of eq. (17). When ΔP_{SR} is zero, i.e., the extrapolated value of ΔP at zero flow rate, the constants C and n can be evaluated by the slope and intercept of ln ΔP plotted versus ln ln (D_b/D_a). Then the constants η and m are evaluated similarly from the plot of ln $(\Delta P - \Delta P_{SH})$ versus ln (Q/D_a^3). These plots showed that the data are correlated satisfactorily by using constant values of the power indices $n = 5$, $m = 2/3$, for all lubricant concentrations and values of the multiplying factors C and η as shown in Table III. The correlation is expressed by

$$\Delta P = 2.53C\,(\ln R)^6 + 4.89\eta[Q \sin^3\alpha/(1 - \cos\alpha)D_b^3]^{2/3}R \quad (26)$$

where ΔP is in psi, Q is in cubic inches/minute, D_b is in inches, and $R = (D_b/D_a)^2$ is the reduction ratio. Equation (26) was obtained by inserting the values of n and m into eq. (17) and simplifying.

TABLE III
Material Constants for Lubricated Teflon 6

Soltrol, %	C	n	η	m
15	0.035	5	3.9	2/3
17	0.026	5	2.2	2/3
19	0.018	5	1.3	2/3
21	0.0086	5	0.9	2/3

By use of eq. (26) the steady-state pressure drop for each of the rheometer experiments was calculated and compared with the experimental value. The comparison is detailed in Table IV and shown graphically for a 19% Soltrol composition in Figure

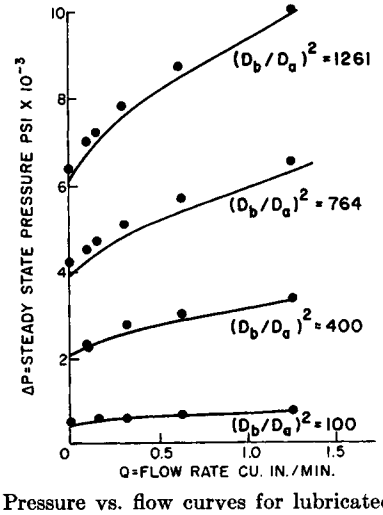

Fig. 7. Pressure vs. flow curves for lubricated Teflon 6. The lines are calculated from eq. (17); points are experimental values.

TABLE IV
Experimental Steady-State Pressure Drop Data Compared with Pressure Drop Calculated from Eq. (7)

Soltrol lubricant, %	Reduction ratio $(D_b/D_a)^2$	Measured and calculated (in parentheses) pressure drop, psi, at various flow rates (in in.³/min.)										
		0.0	0.095	0.11	0.16	0.18	0.32	0.37	0.63	0.74	1.26	1.48
15	764	8600	9400	—	10,800	—	12,000	—	13,200	—	—	—
		(7600)	(8850)	—	(9350)	—	(10,400)	—	(12,000)	—	—	—
	400	4400	4900	—	5250	—	5750	—	6300	—	6900	—
		(4100)	(4750)	—	(5000)	—	(5550)	—	(6400)	—	(7750)	—
	100	700	—	1000	—	1100	—	1150	—	1300	—	1350
		(850)	—	(1050)	—	(1100)	—	(1250)	—	(1500)	—	(1850)
	44.2	500	—	—	—	530	—	—	—	570	—	660
		(250)	—	—	—	(360)	—	—	—	(530)	—	(695)
17	1017	7600	8800	—	9800	—	10,800	—	11,800	—	—	—
		(7250)	(8200)	—	(8550)	—	(9350)	—	(10,550)	—	—	—
	400	2800	3200	—	3400	—	3750	—	4150	—	4800	—
		(3050)	(3400)	—	(3550)	—	(3850)	—	(4350)	—	(5100)	—
	100	600	—	—	—	750	—	—	—	800	—	880
		(650)	—	—	—	(741)	—	—	—	(1000)	—	(1200)
	44.2	300	—	—	—	325	—	—	—	350	—	400
		(200)	—	—	—	(260)	—	—	—	(358)	—	(450)
19	1261	6400	7000	—	7600	—	7800	—	8700	—	9800	—
		(6050)	(6750)	—	(7000)	—	(7600)	—	(8450)	—	(9900)	—
	764	4200	4500	—	4900	—	5100	—	5700	—	6500	—
		(3900)	(4300)	—	(4500)	—	(4850)	—	(5350)	—	(6200)	—
	400	1950	2250	—	2400	—	2750	—	3000	—	3300	—
		(2100)	(2300)	—	(2400)	—	(2600)	—	(2850)	—	(3300)	—
	100	500	530	—	580	—	595	—	635	—	710	—
		(450)	(500)	—	(530)	—	(570)	—	(640)	—	(750)	—
21	1507	2800	3300	—	—	—	4200	—	4500	—	6300	—
		(3350)	(3900)	—	—	—	(4600)	—	(5350)	—	(6500)	—
	1017	2050	—	2750	—	3100	—	3450	—	—	—	4700
		(2400)	—	(2800)	—	(3000)	—	(3350)	—	—	—	(4750)
	764	1800	—	2400	—	2800	—	3100	—	3400	—	4000
		(1850)	—	(2150)	—	(2300)	—	(2550)	—	(3000)	—	(3650)
	400	1200	1350	—	1500	1650	1850	1750	2000	2000	2500	2200
		(1000)	(1150)	—	(1200)	(1250)	(1350)	(1400)	(1500)	(1600)	(1850)	(1950)

7. The fit of the data is generally satisfactory considering that the simple expression used for the viscous resistance contribution of the shearing stress does not allow for any change of viscosity as the lubricant-resin mixture becomes increasingly fibered in the die.

DISCUSSION

The Effect of Die Angle on Extrusion Pressure

Figure 8 shows the effect of changing the (conical) die angle for Teflon 6 and 19% Soltrol paste composition calculated from eq. (17). Two significant aspects of these curves are apparent. Firstly, at zero flow rate dies of the same reduction ratio offer equivalent resistance, ΔP_{SH} irrespective of die angle. Secondly, the smaller the die angle the less extrusion pressure depends on the flow rate. These calculated curves agree in general form with the data of Lewis and Winchester[4] in that experimentally they found pressure to be independent of die angle at low flow rate and also found at finite flow rates that pressure was proportional to die angle. (See Fig. 7 in the Lewis and Winchester paper.[4]) In wire coating where long taper dies (20 or 30° included angle) are used, the dominating effect of the strain-hardening component of pressure sometimes results in experience of failure in attempts to assist an overtaxed piston drive or transmission by reducing the coating speed. The insensitivity of long taper dies to the strain rate can be expected to result in relative insensitivity to local changes of paste consistency (due to poor

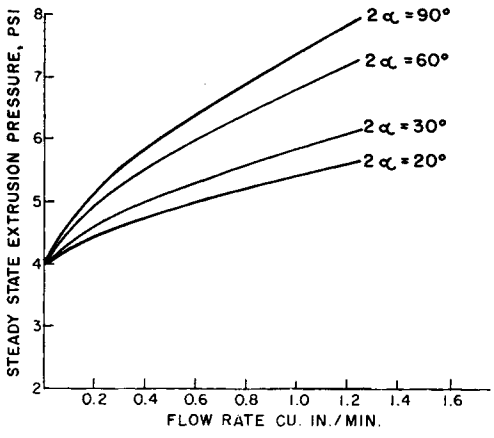

Fig. 8. Effect of die angle: reduction ratio R = 764; 19% Soltrol lubricant. Curves calculated from eq. (17).

blending of lubricant) and therefore a long taper die should give uniform delivery.

The Variation of Pressure to Time of Extrusion

The calculated form of the variation of pressure with time for a constant rate extrusion (Fig. 9) may be divided into two regions, the unsteady-state and steady-state regions. There are two components of pressure, the component due to strain hardening, which reaches its constant maximum value after the discharge of the initial die contents, and the component due to viscous resistance (the strain rate component), which remains constant throughout the extrusion. These regions of extrusion and components of pressure, which may be calculated individually from eq. (11), (13), and (17), are in harmony with observations in commercial and rheometer constant rate extrusions. It is apparent that in extrusions made at constant pressure the pressure must be at least ΔP_{SH} (Fig. 9) or the extrusion will cease before the discharge of the initial die contents. This type of behavior in constant pressure extrusions was observed by Lewis and Winchester,[4] who found that at high pressures the flow rate was essentially constant but at low pressures the flow rate decreased rapidly with time.

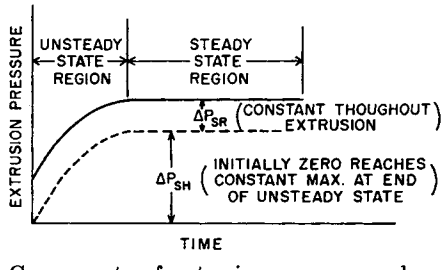

Fig. 9. Components of extrusion pressure and regions of extrusion.

Shearing Stress and Guide Tip Positioning in Wire Coating

The maximum shearing stress at any position in the die may be calculated by use of eq. (18) with the appropriate values of the material constants. This has been done for a 30° angle die and is shown in Figure 10, where τ_{max} and its two components τ_{SH} and τ_{SR} are plotted against reduction ratio. As was seen with extrusion pressure, only the component τ_{SR} can be varied (by changing the extrusion speed) at a particular reduction ratio and paste composition. The component τ_{SH} (fixed by composition and reduction ratio) comprises about 60% of the shearing stress in the example shown.

The high shearing stress values reached at high reduction ratio (Fig. 10) offer a logical explanation of the critical nature of guide tip positioning in

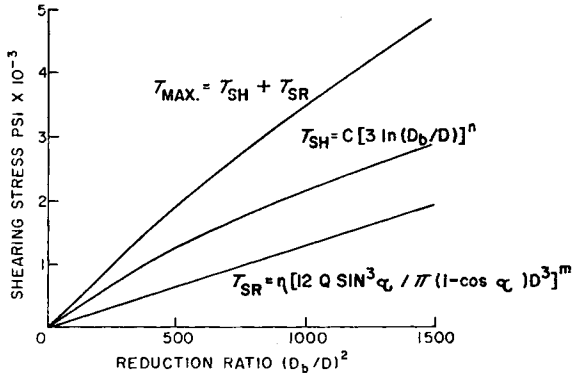

Fig. 10. Shearing stress vs. reduction ratio: for 2α = 30° angle dies at flow; rate Q = 1 in.³/min.

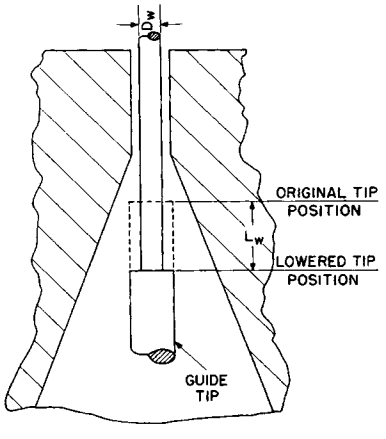

Fig. 11. Lowering wire guide tip.

wire coating at high reduction ratios. It is found that lowering the guide tip by a small amount (Fig. 11) is frequently sufficient to increase the wire tension to the breakage point. This is because lowering the tip exposes an additional length of wire to the lubricant mixture moving more slowly than the wire and the wire shears the paste around it. If a length L_w of solid wire of breaking stress δ_w and diameter D_w is exposed by tip lowering, to paste of shearing strength τ_{max} then the force F shearing the paste around the wire is given by

$$F = \delta_w(\pi D^2/4) = \pi D_w L_w \tau_{max}$$

The length of exposed wire corresponding to a increase of wire stress $\delta\tau$ is, then,

$$L_w = (\delta_w/4\tau_{max})D_w \qquad (27)$$

If, for example, δ_w = 60,000 psi (for copper) and τ_w = 3000 psi, then from eq. (27)

$$L = [60{,}000/(3{,}000 \times 4)]D_w = 5D_w$$

i.e., lowering the guide tip by five wire diameters (about 1/8 in. for hook-up wire) will cause the wire to break.

References

1. Lontz, J. F., J. A. Jaffe, L. E. Robb, and W. B. Happoldt, *Ind. Eng. Chem.*, **44**, 1805 (1952).
2. Thompson, W. B., and R. E. Stabler, *Modern Plastics*, **33**, No. 6, 1115 (1956).
3. De Young, D. N., and G. R. Snelling, *Wire and Wire Products*, **32**, 644 (1957).
4. Lewis, E. E., and C. M. Winchester, *Ind. Eng. Chem.*, **45**, 1123 (1953).
5. Davis, E. A., and S. J. Dolos, *J. Appl. Mech.*, **11**, 193 (1944).
6. Hoffman, O., and G. Sacks, *Theory of Plasticity*, McGraw-Hill, New York, 1953.
7. Jaeger, J. C., *Elasticity, Fracture, and Flow*, Wiley, New York, 1956.
8. Thompson, J. B., G. E. Turrell, and B. W. Sandt, *SPE Journal*, **11**, No. 4, 13 (1955).
9. Allan, A. J. G., *Lubrication Eng.*, **14**, 211 (1958).

Synopsis

For an understanding of the phenomenon of lubricant extrusion of Teflon tetrafluoroethylene resin under nonmelt conditions, a mechanism is proposed based on observed extrusion-hardening and dependence of flow rate on extrusion pressure. These factors can be derived from expressions in which the maximum shearing stress is equated as the sum of two components, one proportional to the maximum shearing strain (strain-hardening component) and another proportional to the strain rate. Thus, in turn, permits the derivation of an expression for the die pressure drop which is in agreement with the experimental data related to flow rate, die dimensions, lubricant concentrations, and time of extrusion. The analysis provides some insight into aspects of commercial extrusion, particularly in wire coating, with practical consideration of the critical nature of guide tip positioning and the effect of wire coating speed on die pressure.

Résumé

Pour obtenir une meilleure compréhension du phénomène d'extrusion lubrifiée du Téflon dans des conditions de nonfusion, on propose un mécanisme basé sur l'observation du durcissement en cours d'extrusion et de la vitesse d'écoulement en fonction de la pression d'extrusion. Ces facteurs peuvent être dérivés d'expressions dans lesquelles le maximum de tension de cisaillement est égalé à la somme de deux composants, l'un proportionnel au maximum de tension (composant de durcissement en cours d'extrusion) et l'autre proportionnel à la vitesse de tension. Ceci permet à son tour la dérivation d'une expression pour la goutte tombante sous pression limite, expression en accord avec les résultats de vitesse d'écoulement, les dimensions limites, les concentrations en lubrifiants et la durée d'extrusion. L'analyse fournit certains points de vue convernant l'extrusion commerciale, en particulier dans le recouvrement des fils, avec des considérations pratiques concernant la position critique de la pointe du guide et l'effet de la vitesse de couvrement des fils sur la pression.

Zusammenfassung

Zum Verständnis der Erscheinung der Schmierstoff-Extrusion von Tetrafluoräthylenharz "Teflon" im nichtgeschmolzenen Zustand wird ein Mechanismus vorgeschlagen der auf der beobachteten Extrusionshärtung und Abhängigkeit der Fliessgeschwindigkeit vom Extrusionsdruck beruht. Diese Faktoren können aus Ausdrücken abgeleitet werden, in welchen die maximale Schubspannung der Summe von zwei Komponenten gleichgesetzt wird, von denen die eine der maximalen Schubdehnung (Dehnungs-Härtungskomponente) und die andere der Dehnungsgeschwindigkeit proportional ist. Dadurch wird wieder die Ableitung eines Ausdrucks für den Druckabfall am Stempel ermöglicht, der mit den experimentellen Daten über Fliessgeschwindigkeit, Stempeldimensionen, Schmierstoffkonzentration und Extrusionsdauer in Übereinstimmung steht. Die durchgeführte Analyse liefert eine gewisse Einsicht in Gesichtspunkte bei der kommerziellen Extrusion, besonders für das Überziehen von Drähten, mit praktischer Betrachtung der kritischen Natur der Stellung der Führungsspitze und des Einflusses der Geschwindigkeit des Drahtüberziehens auf den Stempeldruck.

Received December 21, 1959